Glasses formation, characterization, and crystal-structure determination in the Bi_2O_3–Sb_2O_3–TeO_2 system prepared in an air

Abdeslam Chagraoui · Imane Yakine · Abdelmjid Tairi · Abdenajib Moussaoui · Mohamed Talbi · Mohamed Naji

Abstract A glass-forming domain is found and studied within Bi_2O_3–Sb_2O_3–TeO_2 system. The glasses composition were obtained in pseudo-binary $xSbO_{1.5}$, $(1-x)TeO_2$ for $0.05 \leq x \leq 0.20$. The constitution of glasses in the system Sb_2O_3–TeO_2 was investigated by DSC, Raman, and Infrared spectroscopy. The influence of a gradual addition of the modifier oxides on the coordination geometry of tellurium atoms has been elucidated based Infrared and Raman studies and showed the transition of TeO_4, TeO_{3+1}, and TeO_3 units with increasing Sb_2O_3 content. XRD results reveal the presence of three crystalline: γ-TeO_2, α-TeO_2, and $SbTe_3O_8$ phases during the crystallization process. The density of glasses has been measured. The investigation in the ternary system by the solid state reaction using XRD reveals the existence of a solid solution $Bi_{1-x}Sb_{1-x}Te_{2x}O_4$ isotopic to $BiSbO_4$ with $0 \leq x \leq 0.1$.

A. Chagraoui (✉) · I. Yakine · A. Tairi · A. Moussaoui · M. Talbi
Laboratoire de Chimie Analytique et Physico-Chimie des Matériaux, Faculté des Sciences Ben M'sik, Université Hassan II-Mohammédia, Casablanca, Morocco
e-mail: a_chagraoui@yahoo.fr

M. Naji
CNRS, UPR3079 CEMHTI, 1D avenue de la Recherche Scientifique, 45071 Orléans cedex 2, France

M. Naji
Université d'Orléans, Faculté des Sciences, Avenue du Parc Floral, BP 6749, 45067 Orléans cedex 2, France

Introduction

Tellurium dioxide (TeO_2) is an important material in both amorphous as well as crystalline form and finds application in active optical devices in particular, a huge hyper-susceptibility, deflectors, modulators, γ-ray detectors, and gas sensors because of its high acousto-optic figure of merit, chemical stability, and mechanical durability [1–6]. It is also not hygroscopic and has superior physical properties such as high dielectric constant and low melting point (800 °C) [7–10]. The origin of the extraordinary non-linear optical properties of TeO_2-based glasses is attributed to high hyperpolarizability of a lone electron pair related to the 5 s orbital of tellurium atom. Presently, the well-recognized three modifications of crystalline TeO_2 are α-TeO_2, β-TeO_2, and γ-TeO_2 [11–16]. Of these, recently documented γ-TeO_2 phase has gained a lot of attention for nonlinear optical designs and efforts are made to understand its properties in bulk crystal and glass using as Fourier transform infra-red spectroscopy (FTIR) and Raman spectroscopy. It has been reported that γ-TeO_2 phase appears as the first crystalline structure during the temperature-induced crystallization of TeO_2 glass [17–20]. TeO_2 glass is not stable. An addition of second oxide component M_nO_m makes glasses structures more stable [21–28].

In the present study, we have revisited this system in one hand to obtain more information on the structure of these glasses reported by Charton et al. in Sb_2O_4–TeO_4 system [29, 30]. On the other hand we report the formation, the thermal properties and the local structure using Infrared and Raman studies of glasses prepared in the TeO_2–Sb_2O_3 pseudo-binary and crystalline phases in ternary system. A detailed analysis of the crystalline phase formation in this system synthesized in an oxygen flow will be described successively also.

Experimental procedure

The amorphous and crystalline samples were prepared using high purity commercial materials Bi_2O_3, TeO_2 Sb_2O_3 of analytical grade (Aldrich 99.9%). The batches of suitable proportions of starting products were mixed in an agate mortar and then heated in air at 800 °C (20 min) for vitreous phases and at 600–800 °C (48 h) for crystalline phases. All of them are quenched to room temperature and identified by X-ray diffraction (XRD) using a Bruker D8 Advance diffractometer (Cu-K-alpha radiation). T_g (glass temperature) and T_c (crystallization temperature) were determined using Differential Scanning Calorimetry (DSC) Netsch 2000 PC type from powder samples glasses for about 8 mg in aluminum pans. A heating rate of 10 °C/min was used in the 30–600 °C range. Infrared absorption measurements between 2,000 and 400 cm^{-1} were made for powder specimens dispersed in a pressed KBr disk. The Raman spectra were recorded in the 80–1,000 cm^{-1} range using a Jobin–Yvon spectrometer (64000 model) equipped with an Ar + laser (514.5 nm exciting line) and a CCD detector in a backscattering geometry. The sample focalization was controlled through a microscope (×100). The diameter of the laser spot focused on the sample was about 1 mm. The spectra were recorded in two scans (during 100 s) at low power (<100 mW) of the excitation line, in order to avoid damage of the glasses. The spectral resolution was about 2.5 cm^{-1} at the exciting line. The densities of samples were measured according to the Archimedes principle using diethyl orthophthalate as liquid.

Results and discussion

A wide range glass system based on the Bi_2O_3–Sb_2O_3–TeO_2 system was prepared at 800 °C. This temperature has been chosen to have a homogenous reagent in one hand and to avoid volatilization of TeO_2 at high temperature (T_{TeO_2}Melting = 732 °C) on the other hand (Fig. 1). The color of the glass changes slightly from dark yellow to yellow with increasing Sb_2O_3 and Bi_2O_3 concentration. The glassy domain obtained interval in the pseudo-binary $xSbO_{1.5}$, $(1-x)TeO_2$ $0.05 \leq x \leq 0.20$ is slightly different
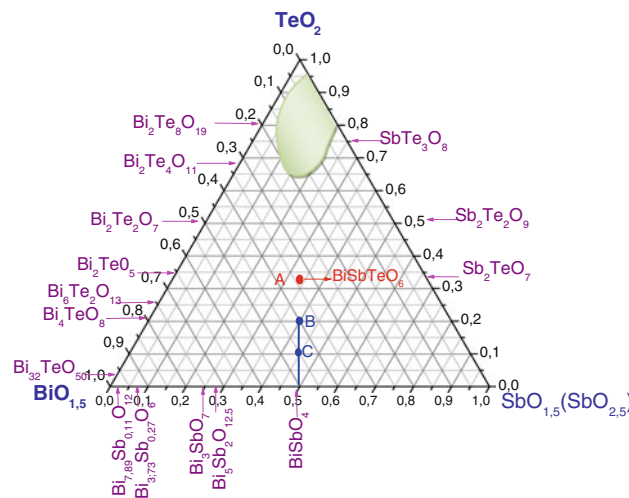
Fig. 1 Phase diagram of Bi_2O_3–$Sb^{(+3,+5)}O_2$–TeO_2 system (colored area = vitreous domain)

to the one proposed by Charton et al. in the xSb_2O_4, $(1-x)$ TeO_2 system study where $0.02 \leq x \leq 0.175$ [29, 30].

Differential scanning calorimetry

Series of glasses composition are listed in Table 1. An addition of $SbO_{1.5}$ (up to 5 mol%) would result in the increase of glass stability (as indicated by $T_c - T_g$). This is presumably due to the participation of Sb^{3+}/Sb^{5+} in the glass network. The values of T_g, T_{c_1}, T_{c_2}, and T_{c_3} are presented (Fig. 2 and Table 1).

The DSC curves exhibit an endothermic effect due to glass transition (T_g). At higher temperatures three exothermic peaks are observed and related to temperature crystalline phases. Figure 2 shows the dependence of characteristic temperature, glass transition, the first crystallization (T_{c_1}), the second (T_{c_2}), and the third crystallization (T_{c_3}) on Sb_2O_3 content. The appearance of single peak (all glasses) due the glass transition temperature indicates the homogeneity of the glasses prepared. With increasing in the concentration of Sb_2O_3 in the glass matrix, the T_g increases and the difference ($T_c - T_g$) (about 77–98 °C) implies a thermal stability of glasses. In a study of alkali tellurite glasses, Pye et al [31] showed that the temperature of the glass transition decreases with increasing amount of Li, Na, or K compound. The dependence of Sb_2O_3 content shows a different tendency

Table 1 Glass composition, their respective thermal parameter, density and molar volume

| % mol TeO$_2$	% mol SbO$_{1.5}$	T_g (°C)	T_{c_1} (°C)	T_{c_2} (°C)	T_{c_3} (°C)	$T_{c_1} - T_g$	Density ($\pm$0.02) g/cm^3	Molar volume (cm^3/mol)
95	5	328	405	497	573	77	5.95	27.93
90	10	329	409	519	571	80	6.00	28.80
85	15	334	430	509	575	96	6.10	29.40
80	20	339	437	500	563	98	6.18	30.09
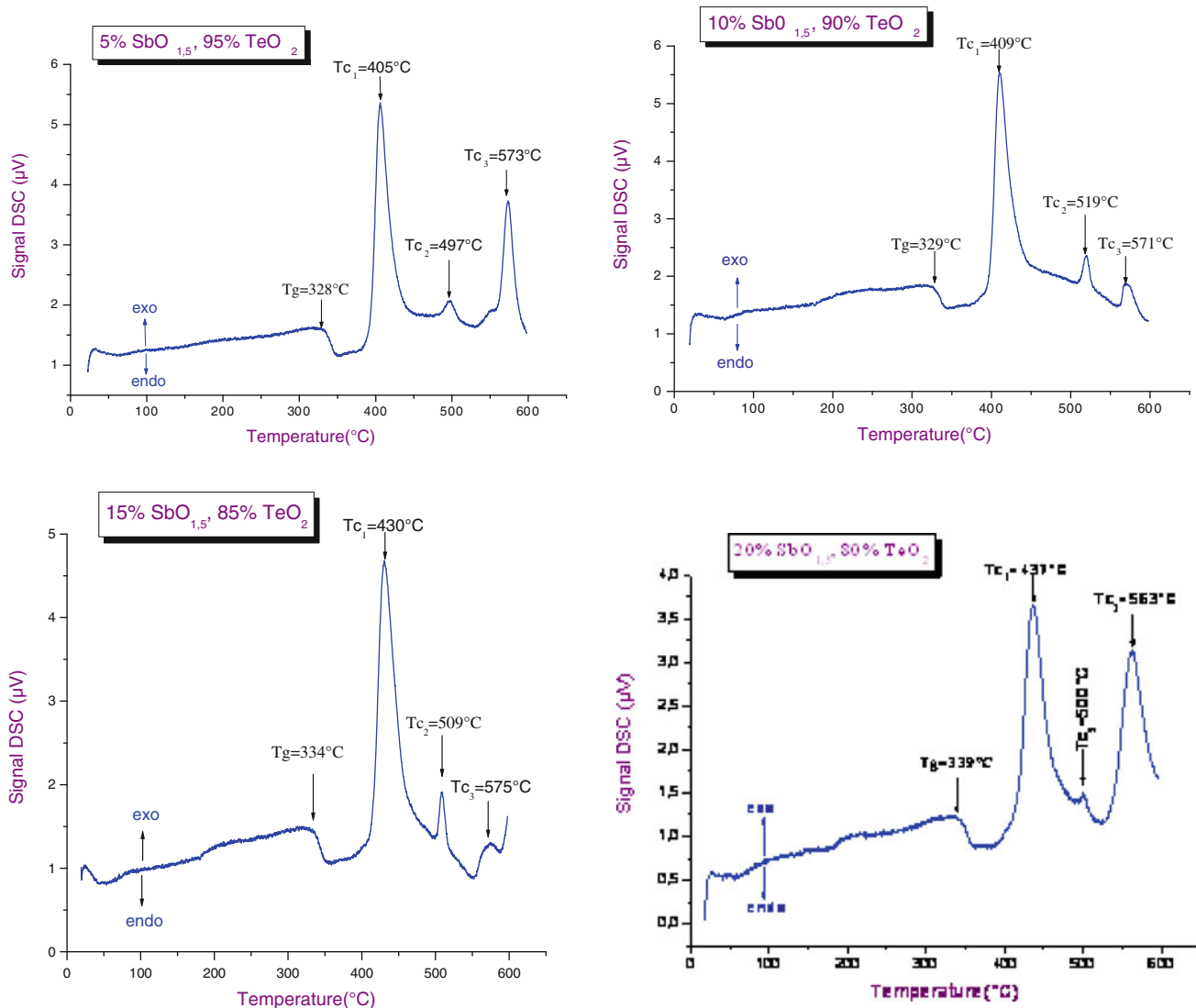
Fig. 2 DSC curves of glassy samples obtained in $(1-x)$TeO$_2$, xSbO$_{1.5}$ pseudo- binary $(0.05 \leq x \leq 0.20)$

especially of glass transition compared with the alkali tellurite glasses. The alkali atoms easily move in the glass structure. However, antimony atoms move with greater difficulty in the glass, because the Sb atom is restrained by relatively strong bonds to every coordinate oxygen. The slight change of the temperature of crystallization of a vitreous composition to another is due to the kinetic phenomenon. Based on XRD and DSC analysis for glassy samples 5–20 mol% SbO$_{1.5}$ (see Fig. 3) a first peak of crystallization corresponds to the γTeO$_2$, αTeO$_2$, and SbTe$_3$O$_8$ at 405–437 °C range. This phenomenon which we observed the crystallization γTeO$_2$ variety could be expected: similar behavior has been observed in the many others systems as TeO$_2$–WO$_3$ [15], Nb$_2$O$_5$–TeO$_2$ [13, 16], TeO$_2$–ZnO [18] and TeO$_2$–SrO [19]. In second crystallization ranging 497–519 °C belongs to reinforcing SbTe$_3$O$_8$ and TeO$_2\alpha$ phases. The last peak

(563–573 °C) with weak intensity is attributed to totally transformation γTeO$_2$ metastable polymorph into the stable αTeO$_2$ and SbTe$_3$O$_8$. It can be observed that there is a linear relationship between $T_c - T_g$ and T_c against the Sb$_2$O$_3$ content. This indicates that the glass is easily fabricated. The increase in glass stability is also reported to be due to the structural formation of SbTe$_3$O$_8$ units.

Density

The density of the specimens was measured using Archimeds principle using orthophtalate as the immersion liquid ($d_{orthophtalate} = 1.11712$ at 22 °C). A glass disc was weighted in air (W_{air}) and immersed in orthophtalate and reweighted ($W_{orthophtalate}$). The relative density is given by the following relation [22]:
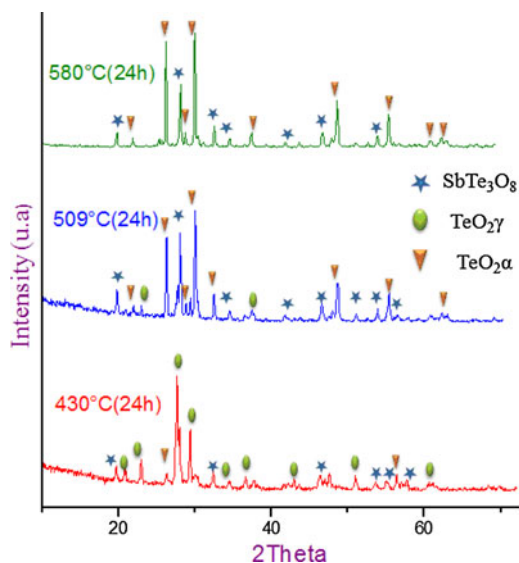
Fig. 3 XRD patterns heat-treated at 430 °C, 509 °C and 580 °C of (90% TeO_2, 10% $SbO_{1.5}$ mol) in pseudo-binary TeO_2–$SbO_{1.5}$

$$d = d_{\text{orthophtalate}} \frac{W_{\text{air}}}{W_{\text{orthophtalate}}}$$

In pseudo-binary, the glass density increases with the augmentation of $SbO_{1.5}/TeO_2$.

From the result (see Table 1), it can be seen that values of density increase with the addition of Sb_2O_3 is obviously due the difference of Sb and Te atoms weights.

Infrared spectroscopy

The infrared spectra transmission of glasses compositions are given in Fig. 4. A tellurite network basically consists of TeO_4 trigonal bipyramids (TBP) units and TeO_3 trigonal pyramid (TP) units, each of which has a lone pair of electrons, while the constitution of binary glasses depends on the second metal oxides. Suzuki [33] reported that TBP units were converted to TP ones on barium and sodium tellurite glasses. He proposed a mechanism (Eqs. 1 and 2) of the formation of the TP units:

$$3TeO_{4/2} + O^{2-} \rightarrow O_{2/2}Te-O + 2TeO_{3/2}O^- \quad (1)$$

$$O_{2/2}Te-O + 2TeO_{3/2}O^- + 2\,O^{2-} \rightarrow 3TeO_3^{2-} \quad (2)$$
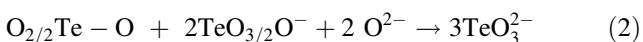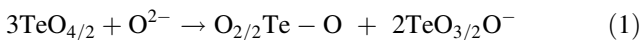
where $O_{1/2}$ represents bridging oxygen. These two reactions proceed as the content of a network modifying oxide increases until all the oxygen atoms of the (TBP) units become non-bridging (Eq. 3).

$$TeO_{4/2} + O^{2-} \rightarrow TeO_3^{2-} \quad (3)$$

The three oxygens in the TeO_3^{2-} units are equivalent.

The TeO_2 glass ($x = 0$) infrared spectrum is rather similar to αTeO_2 data including the typical broadening
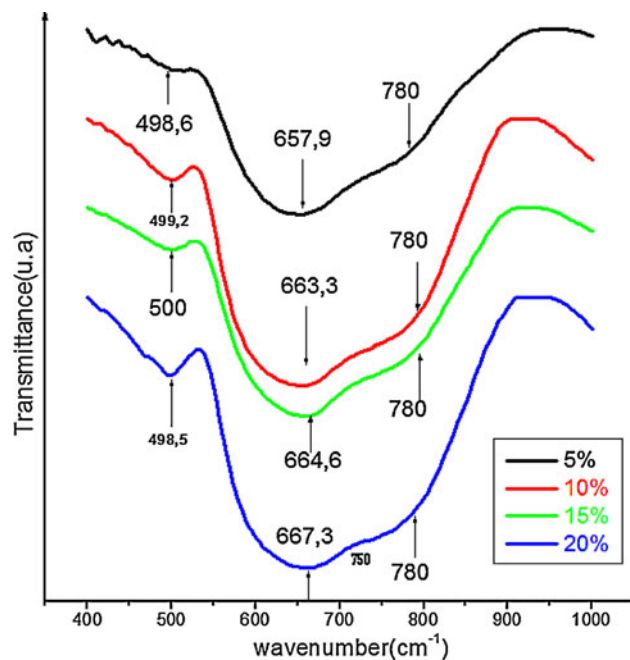
Fig. 4 Infrared spectra of $(1-x)\ TeO_2,\ xSbO_{1.5}$ with $(0.05 \leq x \leq 0.20)$

observed in glasses. TeO_2 vitrification is thus characterized by a redistribution of infrared intensities due to spatial rearrangement of TeO_4E units involving a decrease of TeO_4E units symmetry which explains that the band at 625 cm^{-1} becomes predominant [33]. As the Sb_2O_3 proportion increases (Fig. 4), the major band shifts from 625 cm^{-1} ($x = 0$) to 667 cm^{-1} ($x > 0.05$) which is attributed to TeO_3E trigonal pyramid. The presence of shoulder around 780 cm^{-1} for all studied glass compositions is the signature of TeO_4E trigonal pyramid. For $x = 0.20$ we observed a band at 750 cm^{-1} nearly which attributed to TeO_{3+1} group. The absorption band nearly 500 cm^{-1} which slightly increases in intensity with Sb_2O_3 content can be assigned to Te–O–Te and Te–O–Sb bridging bonds which would increase the network connectivity in agreement with th T_g increase. On the other hand, from the reference spectra lithium tellurite glasses the infrared broad absorption sharp bands at around 610 cm^{-1} are attributed to group vibration of TeO_6 [21, 34]; Therefore in our preparation glasses, we do not observed this band so there is no oxidation of Te^{+4} to Te^{+6}.

Raman spectra

In tellurite glasses, XANES, X-ray absorption and Raman spectroscopy previously showed that tellurium is surrounded by oxygen atoms and generally localized in three types of sites with different geometries. For the lowest amounts of additional oxides the dominant tellurium site

are [TeO$_4$] trigonal bipyramids which are axially elongated and partly connected to each other sharing one oxygen atom. When increasing the amount of additional oxides they progressively convert into [TeO$_3$] regular trigonal pyramids via [TeO$_{3+1}$] entities where one axial Te–O$_{ax}$ distance is elongating while the others shortens getting closer to the shortest equatorial Te–O$_{eq}$ distances [25, 28–30, 35–41].

The Raman spectra of xSbO$_{1.5}$, $(1-x)$ TeO$_2$ $(5 \leq x \leq 20\% \text{ mol})$ glasses are shown in Fig. 5a. For all samples, spectra obtained from different spots are identical showing high homogeneity of glasses. They are two pronounced peaks occur around 640–670 and 760–770 cm^{-1}. The most prominent band at 659 cm^{-1} in the spectrum of pure glass is related to the combined vibrations of asymmetric stretching of Te$_{eq}$–O$_{ax}$–Te bonds and symmetric stretching of TeO$_4$ (TBP). With addition of SbO$_{1.5}$ up 20% mol fraction, intensity of this band decreases (G1), while bands at 760–768 cm^{-1} (G2) attributed to stretching vibrations of non-bridging Te–O– bands in TeO$_3$ (TP). The peak (G2), which is assigned to a stretching vibration of TeO$_4$ units, was observed to decrease as the Sb$_2$O$_3$ contents increases. The decrease in intensity would suggest the possibility of conversion from TeO$_4$ TBP units to the other basic structural unit [37]. The peak (G1) is reported to be due to the perturbation of TeO$_4$ (TBP) units into TeO$_3$ (trigonal pyramids) units via the intermediate coordination of TeO$_{3+1}$ [34, 35, 37]. Both features would clearly indicate that the network of the TeO$_3$ structural unit increases with the increasing of Sb$_2$O$_3$ contents. Other peaks around (P) 452–456 cm^{-1} are observed to be less sensitive to the Sb$_2$O$_3$ contents. Antimony atoms are incorporation in the glass implied the formation of Te–O–Sb bridging bonds which stabilizes the glass formation in accordance with $T_c - T_g$ increase. A decrease in the peak intensity would suggest the occurrence of the destruction of Te–O–Te (or O–Te–O) in the linkages, thus resulted in the decreasing of the Te–O–Te linkages in a continue network of TeO$_n$ $(n = 4, 3 + 1, \text{ or } 3)$ entities, which is consistent with the observation reported elsewhere [35], the intensity of this band decreases, while bands at 760 and 769 cm^{-1} were attributed to stretching vibrations of non-bridging Te–O– bands in TeO$_3$ (TP) grow in intensity.

The spectral deconvolution of binary glasses indicates that five strong bands are present at about 450–767 cm^{-1}. The bands are mainly attributed to the vibrations of coordination polyhedra of tellurium atoms. Figure 5b and Table 2 show results of band deconvolution of the spectra of xSbO$_{1.5}$, $(1-x)$ TeO$_2$ $(5 \leq x \leq 20\% \text{ mol})$. A good agreement was obtained between the observed and simulated spectra. The fitting of the spectra was made with focus, a curve fitting soft wave especially adapted for analysis of optical spectra [42].
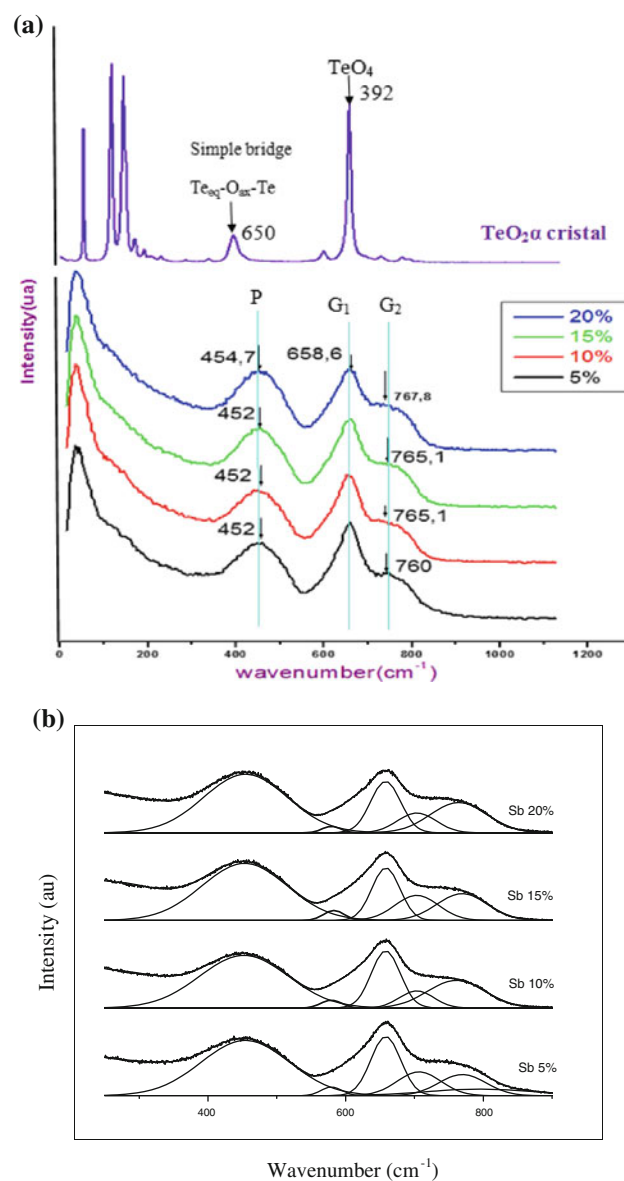
Fig. 5 a Raman spectra of glasses and crystalline phases of $(1-x)$ TeO$_2$, xSbO$_{1.5}$ with $(0.05 \leq x \leq 0.20)$ in the TeO$_2$–Sb$_2$O$_3$ system. **b** Deconvolution of Raman spectra for $(1-x)$ TeO$_2$, xSbO$_{1.5}$ with $(0.05 \leq x \leq 0.20)$

The orthotellurate ion, TeO$_6^{6-}$, will have octahedral symmetry but may be strongly distorted. Vibrational modes for the tellurate anion should occur in the 620–650 cm^{-1} and in the 290–360 cm^{-1} regions [43]. In our spectrum, these intense bands do not appear, therefore there is no Te^{6+} in our vitreous composition.

Crystalline phases

A solid state investigation of the Bi$_2$O$_3$–Sb$_2$O$_3$–TeO$_2$ system allowed synthesis of crystalline phases SbTe$_3$O$_8$ and

Table 2 Wave number of the Raman spectra for $(1-x)$ TeO_2, $xSbO_{1.5}$ $(0.05 \leq x \leq 0.20)$

Compositions	Wave number (cm^{-1})	Intensity
$x = 0.05$	456.778 (P)	1.39923
	614.958	0.822273
	658.375 (G1)	1.61736
	706.841	0.656697
	769.854 (G2)	0.589822
$x = 0.1$	454.85 (P)	1.33616
	615.501	0.834616
	658.321 (G1)	1.56564
	703.273	0.477487
	761.015 (G2)	0.772023
$x = 0.15$	455.516 (P)	1.44533
	618.24	0.865094
	658.542 (G1)	1.43989
	703.606	0.692268
	769.476 (G2)	0.74740
$x = 0.2$	456.836 (P)	1.48301
	614.482	0.788364
	658.103 (G1)	1.40338
	703.506	0.547722
	764.53 (G2)	0.842251

Fig. 6 XRD patterns of $Bi_{1-x}Sb_{1-x}Te_{2x}O_4$ solid solution with $0 \leq x \leq 0.1$

$Sb_2Te_2O_9$ which have been obtained at 600–750 °C in air and characterized by XRD.

$SbTe_3O_8$

This phase, is characterized by powder diffraction X and indexed in the cubic system with parameter $a = 11.025(2)$ Å. No significant change in weight was observed, result implies no oxidation of Te^{IV}. This phase derived from fluorine phase is seems isotropic to $TiTe_3O_8$ [44] and its structure determination well be published.

$Sb_2Te_2O_9$

This phase is obtained from 2 mol TeO_2 and 1 mol Sb_2O_3. The mass gain during the synthesis of this compound was observed, which is probably related to an increase in

oxygen content due to the oxidation of Te^{4+} to Te^{6+} and/or Sb^{3+} to Sb^{5+}. Using the 11 most intense reflections of X-ray diffraction powder pattern, the indexing program dicvol [45] yielded monoclinic symmetry. All observed reflections were indexed and the figures merit were M20 = 38. After a least-squares refinement, the cell parameters were: $a = 21.466(1)$ Å, $b = 4.903(1)$ Å, $c = 14.469(1)$ Å; $\beta = 110.89(1)°$. These parameters were good agreement as reported in the ICDD files n°79-2317.

Analysis by diffraction X of Bi_2O_3–TeO_2–$Sb_2O_3(Sb_2O_5)$ system

A series of compositions in the system of carefully chosen and were treated at different temperatures between 600 and 800 °C. Their analysis by X-ray diffraction revealed the existence of a stable phase $BiSbO_4$ [46] and other phases localized in Bi_2O_3–TeO_2 or Bi_2O_3–$Sb_2O_3(Sb_2O_5)$ pseudo-binary. Typical X-ray diffraction patterns of $Bi_{1-x}Sb_{1-x}Te_{2x}O_4$ $0 \leq x \leq 0.5$ are shown in (Fig. 6). Solid solution of $Bi_{1-x}Sb_{1-x}Te_{2x}O_4$ exist for the range $(0 \leq x \leq 0.1)$ (compositions B and C) and the lattice parameters from XRD pattern are listed in Table 3. They are compared to $BiSbO_4$ phase. We find that the coupled substitution of antimony and bismuth atoms in size by the average of tellurium in the network and has no significant influence on

Table 3 Parameters evolution of $Bi_{1-x}Sb_{1-x}Te_{2x}O_4$ solid solution with $0 \leq x \leq 0.1$

Composition: $Bi_{1-x}Sb_{1-x}Te_{2x}O_4$	Cell parameters	Volume (± 0.02 Å)^3
$x = 0$: $BiSbO_4$	$a = 5.469(1)$ Å, $b = 4.8847(1)$ Å $c = 11.8285(1)$ Å, $\beta = 101.13°(1)$	309.96
$x = 0.05$: $Bi_{0.95}Sb_{0.95}Te_{0.1}O_4$	$a = 5.469$ Å(1), $b = 4.887(1)$ Å $c = 11.822(1)$ Å, $\beta = 101.12°(1)$	310.05
$x = 0.10$: $Bi_{0.9}Sb_{0.9}Te_{0.2}O_4$	$a = 5.466$ Å(1), $b = 4.884(1)$ Å $c = 11.825(1)$ Å, $\beta = 101.19°(1)$	309.75

the evolution of lattice parameters. Phase up to $x = 0.5$ ($BiSbTeO_4$) (A) adopt the $Bi_2Te_2O_7$ and the limit solid solution.

Remarks

Owing to the oxidation of Sb^{+3} and Te^{+4}, the investigated Bi_2O_3–Sb_2O_3–TeO_2 system cannot be considered as a ternary, but rather as a pseudo-quaternary $Bi^{3+}/Te^{+4}/Te^{+6}/Sb^{+3}/Sb^{+5}$ system. Our investigation of the Bi_2O_3–Sb_2O_3–TeO_2 system revealed the important influence of the oxygen atmosphere on the chemistry and the crystallography of the phases found.

Conclusions

In the Bi_2O_3–Sb_2O_3–TeO_2 pseudo-ternary system, stable and transparent glasses were been synthesized at 800 °C. The vitreous domain in pseudo-binary $(1-x)TeO_2$–$xSbO_{1.5}$ system is: $0.05 \leq x \leq 0.2$. Its characteristic temperatures (glass transition and crystallization temperatures) have been determined. The crystallization of the samples rich of TeO_2 occurs for the γTeO_2, Te_3SbO_8 and αTeO_2. The γTeO_2 variety transforms complete to αTeO_2 up 500 °C. The IR and Raman spectra of glasses were interpreted in terms of structural transformations produced by modifiers; from TeO_4 trigonal bipyramid to TeO_3 trigonal pyramid via $[TeO_{3+1}]$ entities with increasing of the Sb_2O_3 content in glass. The formation Sb–O–Te linkages and 3-fold coordinated oxygen atoms which increase the polymerization of the glass network in accordance with an increase of the glass transition temperature which proportion depends on composition. A solid state investigation by X-ray of the system allowed Te_3SbO_8, where no oxidation of Te^{4+} to Te^{6+} is allowed by synthesizing in oxygen atmosphere and the Sb atoms present is a mixed oxidation state, Sb^{3+} and Sb^{5+}. In the $Sb_2Te_2O_9$ phase, the antimony and tellurium atoms are in Sb^{5+} and Te^{6+} state, respectively. The densities of the glasses increase in Sb_2O_3 content. The investigation by X-ray diffraction in the ternary system allowed the existence a solid solution with the formulation $Bi_{1-x}Sb_{1-x}Te_{2x}O_4$ isotopic to $BiSbO_4 : 0 \leq x \leq 0.1$.

Open Access This article is distributed under the terms of the Creative Commons Attribution Noncommercial License which permits any noncommercial use, distribution, and reproduction in any medium, provided the original author(s) and source are credited.

References

1. Abdulhalim I, Pannel CN, Wang J, Wylangowski G, Payne DN (1994) J Appl Phys 75:519
2. Yano T, Fukumoto A, Watanabe A (1971) J Appl Phys 42:3674
3. Kotov VM, Shkerdin GN, Shkerdin DG, Kotov EV (2005) J Opt Technol 72:511
4. Takenaga M, Yamada N, Nishiuchi K, Akahira N, Ohta T, Nakamura S, Yamashita T (1983) J Appl Phys 54:5376
5. Arshak K, Korostynska O (2002) Sensors 2:347
6. Sen S, Muthe KP, Joshi N, Gadkari SC, Gupta SK, Jagannath M, Roy M, Deshpande SK, Yakhmi JV (2004) Sensors Actuators B 98:154
7. El-Mallawany R (1992) J Appl Phys 72:1774
8. Kim SH, Yoko T, Sakka S (1993) J Am Ceram Soc 76:2486
9. El-Mallawany RAH (2001) Tellurite glasses handbook. CRC Press, Boca Raton, p 113
10. Nasu H, Matsushita O, Kamiya K, Kobayashi H, Kubodera K (1990) J Non-Cryst Solids 124:275
11. Thomas PA (1988) J Phys C 21:4611
12. Beyer VH (1967) Zeitschrift für Kristallographie 124:228
13. Blanchandin S, Marchet P, Thomas P, Champarnaud-Mesjard J-C, Frit B (1999) J Mater Chem 9:1785
14. Champarnaud-Mesjard J-C, Blanchandin S, Thomas P, Mirgodsky AP, Merle-Mejean T, Frit B (2000) J Phys Chem Solids 61:1499
15. Blanchandin S, Thomas P, Marchet P, Frit B, Chagraoui A, Mater J (1999) Sciences 34:4285
16. Blanchandin S, Thomas P, Marchet P, Champarnaud-Mesjard JC, Frit B (2002) J Alloys Compd 34:206
17. Dewan N, Sreenivas K, Gupta V (2007) J Cryst Growth 305:237
18. Chagraoui A, Chakib A, Mandil A, Tairi A, Ramzi Z, Benmokhtar S (2007) Scripta Materialia 56:93
19. Chagraoui A, Ramzi Z, Tairi A, Mandil A, Talibouridah M, Ajebli K, Abboud Y (2009) J Mater Process Technol 209:3111
20. Chagraoui A, Bensaid H, Tairi A, Ajebli K, Moussaoui A (2010) J Alloys Compd 495:67
21. Idalgo E, Ara′ujo EB, Yukimitu K, Moraes JCS, Reynoso VCS, Carvalho CL (2006) Mater Sci Eng A 434:13
22. Sidek HAA, Hamezan M, Zaidan AW, Talib ZA, Kaida K (2005) Am J Appl Sci 2(8):1266
23. Sekiya T, Mochida N, Soejima A (1995) J Non-Cryst Solids 19i:115
24. Rosmawati S, Sidek HAA, Zainal AT, Mohd Zobir H (2008) J Appl Sci 8(10):1956
25. Rong QJ, Osaka A, Nanba T, Takada J, Miura Y (1992) J Mater Sci 27:3793. doi:10.1007/BF00545458
26. Udovic M, Thomas P, Mirgorodsky A, Masson O, Merle-Mejean T, Lasbrugnas C, Champarnaud-Mesjard JC, Hayakawa T (2009) Mater Res Bull 44:248
27. Chen Y, Nie Q, Xu T, Dai S, Xang X, Shen X (2008) J Non-Cryst Solids 354:3468
28. Soulis M, Mirgorodsky AP, Merle-Mejean T, Masson O, Thomas P, Udovic M (2008) J Non-Cryst Solids 354:143
29. Charton P, Armand P (2003) J Non-Cryst Solids 316:189
30. Charton P, Thomas P, Armand P (2003) J Non-Cryst Solids 321:81
31. Pye LD, Stevens HJ, Lacourse WC (1992) The physics of non-crystalline solids. Taylor and Francis, London, p 281
32. Blanchandin S, Thomas P, Marchet P, Champarnaud-Mesjard JC, Frit B (1999) J Mater Chem 9:1785
33. Suzuki K (1987) J Non-Cryst Solids 95/96:15
34. Sekiya T, Mochida N, Ohtsuka J, Tonokawa M (1989) Nippon Seramikkusu, Kyokai Gakujutsu Ronbunshi 97:1435
35. Nazabal V, Todoroki S, Nukui A, Matsumoto T, Suehara S, Hondo T, Araki T, Inoue S, Rivero C, Cardinal T (2003) J Non-Cryst Solids 325:85
36. Kawasaki S, Honma T, Benino Y, Pujiwara T, Sato R, Komatsu T (2003) J Non-Cryst Solids 325:61
37. Li H, Su Y, Sundaram SK (2001) J Non-Cryst Solids 293–295:402

38. Sabadel Armand JC, Cachau-Herreillat D, Baldeck P, Doclot O, Ibanez A, Philippot E (1997) J Solid State Chem 132:411
39. Komatsu T, Tawarayama H, Mohri H, Matusita K (1991) J Non-Cryst Solids 135:105
40. Hu L, Jiang Z (1996) Phys Chem Glasses 37(1):19
41. Dimitrova-Pankova M, Dimitriev Y, Arnaudov M, Dimitrov V (1989) Phys Chem Glasses 30(6):260
42. Focus web site.<http://crmht.cnrs-orleans.fr/pot/software/focus.html>
43. Frost RL, Keeffe EC (2009) J Raman Spectrosc 40:249
44. Bindi L, Cipriani C (2003) Can Mineral 41:1469
45. Boultif A, Louer D (1991) J Appl Crystallogr 24:987
46. Kennedy, Brendy J (1994) Powder Diffr 9:164